TASK QUARTERLY 15 No 3–4, 271–282

NUMERICAL SIMULATION OF OPEN CHANNEL FLOW BETWEEN BRIDGE PIERS

MICHAŁ SZYDŁOWSKI

Faculty of Civil and Environmental Engineering,
Gdansk University of Technology,
Narutowicza 11/12, 80-233 Gdansk, Poland
michal.szydlowski@wilis.pg.gda.pl

(Received 10 May 2011; revised manuscript received 2 August 2011)

Abstract: Free-surface flow in the vicinity of bridge piers on a fixed channel bed is a classical problem of open-channel hydraulics. This problem is usually analyzed using one-dimensional hydraulic models for steady-flow problems. The aim of this paper is to present a two-dimensional numerical simulation of water flow around obstacles, such as cylinders, which can act as a simplified model of real piers. The depth-averaged Navier-Stokes equations describing unsteady free-surface flow are solved using an explicit scheme of the finite-volume method. The numerical solution prepared for the simulations of unsteady free-surface flows was used here to analyze the case of steady flow. A numerical simulation of flow in the channel with the obstruction was performed for two different inflow discharges determining, respectively, the subcritical and supercritical flow in the cross-section of a channel constriction. In the second simulation, a hydraulic jump was observed downstream of the bridge section. The numerical results were compared with measurements. Water surface profiles were measured for both discharges in the hydraulic laboratory of the Faculty of Civil and Environmental Engineering at Gdansk University of Technology (GUT). Comparisons with laboratory data showed that the proposed approach constitutes a sufficiently accurate and reliable technique for predicting basic flow parameters. The method of two-dimensional modeling of flow in a river channel between bridge piers can be also integrated with the simulation of unsteady flood wave propagation, ensuring a uniform approach to the problem of flood modeling in river valleys. Moreover, a two-dimensional simulation yields detailed information about flow structure near the obstruction, which can be used to better elucidate debris transport and river bed deformation processes.

Keywords: mathematical modeling, numerical simulation, open channel flow, bridge piers

1. Introduction

Free-surface flow between bridge piers is a classical problem of open-channel hydraulics [1]. Bridge piers can be treated as a short obstruction in a channel, resulting in a constriction (sudden reduction of the channel cross-section). The

classical one-dimensional theory of flow through a non-prismatic channel section was clearly described by Chow [2]. The effect of the constriction depends mainly on the channel geometry, flow discharge, and the state of flow, which can be sub- or supercritical. In a channel with a mild slope, the flow is usually subcritical. If the constriction is limited, the obstruction induces a backwater effect, which may extend over a long distance upstream, in which case the flow is subcritical both along the constriction and in the downstream channel. However, if the relative constriction is longer, it forms a short channel, which may cause the minimum value of specific energy to rise in the constriction section, corresponding to the critical stage. This results in the development of supercritical flow, which can return to normal conditions by a hydraulic jump. Different effects can be observed in steep slope channels under the conditions of supercritical flow. When the flow is supercritical, the constriction disturbs only the water surface adjacent to the upstream side of the constriction. If the constriction is limited, only the water surface close to the constriction is disturbed and the effect does not extend further upstream. However, if the constriction is significant it can make the depth upstream of the constriction greater than the critical depth, as the specific energy upstream of the obstruction must increase. This makes the flow subcritical in this channel section and requires the formation of a hydraulic jump. The swelling of the water surface extends only over a short section of the upstream construction.

The theoretical one-dimensional description of the influence of the channel constriction provides only the information about the parameters of steady flow along the channel. If a more complex analysis of the flow structure near the cross-section of a bridge is needed, multi-dimensional modeling must be employed. The required complexity of the model is determined by the aim of the numerical simulation. For instance, for the analysis of local scour of a river bed near bridge piers full three-dimensional turbulent flow modeling combined with a sediment transport model must be performed [3, 4]. The same model should be used for the simulation of the entire structure of local hydraulic phenomena. However, for the simulations of river flow, valley inundations and other water management problems, *i.e.* when the inner structure of local effects is not essential for the hydraulic analysis, two-dimensional (depth-averaged) hydrodynamic models are usually sufficient [5]. In order to integrate the model of the flow between bridge piers with a flood modeling system, the shallow-water equations were used to describe the motion of water through the channel with an obstruction. Numerical simulations were compared with laboratory measurements of the water surface profile. In order to carry out the experiment, a simplified model of the bridge section was prepared in a laboratory channel. The comparison between the computed and measured data is presented subsequently in this paper.

2. Numerical model of two-dimensional open-channel flow

A system of shallow water equations (SWEs) in conservation form can be written as [6]:

$$\frac{\partial \boldsymbol{U}}{\partial t}+\frac{\partial \boldsymbol{E}}{\partial x}+\frac{\partial \boldsymbol{G}}{\partial y}+\boldsymbol{S}=0 \tag{1}$$

where

$$\boldsymbol{U}=\begin{pmatrix} h \\ uh \\ vh \end{pmatrix}, \qquad \boldsymbol{S}=\begin{pmatrix} 0 \\ -gh(S_{ox}-S_{fx}) \\ -gh(S_{oy}-S_{fy}) \end{pmatrix} \tag{2}$$

$$\boldsymbol{E}=\begin{pmatrix} uh \\ u^2h+0.5gh^2 \\ uvh \end{pmatrix}, \qquad \boldsymbol{G}=\begin{pmatrix} vh \\ uvh \\ v^2h+0.5gh^2 \end{pmatrix} \tag{3}$$

In this system of equations, h is the water depth, u and v are the depth-averaged components of velocity in the x and y direction, respectively, S_{ox} and S_{oy} denote the bed slope terms, S_{fx} and S_{fy} are the bottom friction terms defined by the Manning formula, and g is the acceleration due to gravity. Equation (1) can also be written as:

$$\frac{\partial \boldsymbol{U}}{\partial t}+\operatorname{div}\boldsymbol{F}+\boldsymbol{S}=0 \tag{4}$$

where, assuming a unit vector $\boldsymbol{n}=(n_x,n_y)^T$, the vector $\boldsymbol{F}$ is defined as $\boldsymbol{F}\boldsymbol{n}=\boldsymbol{E}n_x+\boldsymbol{G}n_y$.

In order to spatially integrate the SWEs using the finite volume method (FVM), the calculation domain was discretized into a set of triangular cells (Figure 1) [5].

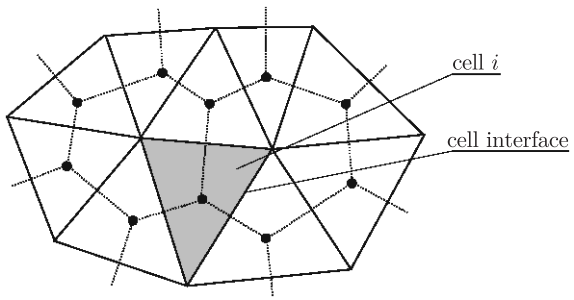

Figure 1. Triangular computational cells for the FVM

Following integration and replacement of integrals by the corresponding sums, Equation (4) can be rewritten as:

$$\frac{\partial \boldsymbol{U}_i}{\partial t}\Delta A_i+\sum_{r=1}^{3}(\boldsymbol{F}_r\boldsymbol{n}_r)\Delta L_r+\sum_{r=1}^{3}\boldsymbol{S}_r\Delta A_r=0 \tag{5}$$

where $\boldsymbol{F}_r$ is the numerical flux (computed at the r^{th} cell interface) and ΔL_r is the length of the cell interface. $\boldsymbol{S}_r$ and ΔA_r are the components of the source terms and the area of cell i assigned to the r^{th} cell interface, respectively. In order to

calculate the fluxes $\boldsymbol{F}_r$, the solution of the approximated Riemann problem was used. A description of the method was presented in [7, 8]. The source term vector $\boldsymbol{S}$ contains two types of elements depending on the bottom and friction slopes, respectively. In order to avoid numerical integration, the splitting technique for physical processes is applied. The numerical algorithm is complemented by a two-stage explicit scheme of time integration.

3. Laboratory experiments

The experimental set-up was built in the hydraulic laboratory at Gdansk University of Technology. The tests were carried out in a rectangular open channel with a concrete bed and glass walls. The total length of the set-up was about 28 m. The active segment of the laboratory channel (with glass walls) was 15 m long and 0.62 m wide. The bridge model section was located 2 m downstream of the inflow section. There were two circular piers with a diameter of 0.11 m. The distances between the channel walls and the piers and between the piers were identical and measured 0.134 m. A schematic and photographs of the laboratory channel are presented in Figures 2 and 3. The water surface profiles along the channel were measured using a gauging needle. The ordinates of the water surface were determined along the channel axis and along the pier axis in a stretch ranging from about 1 m upstream to 1.5 m downstream of the bridge model.

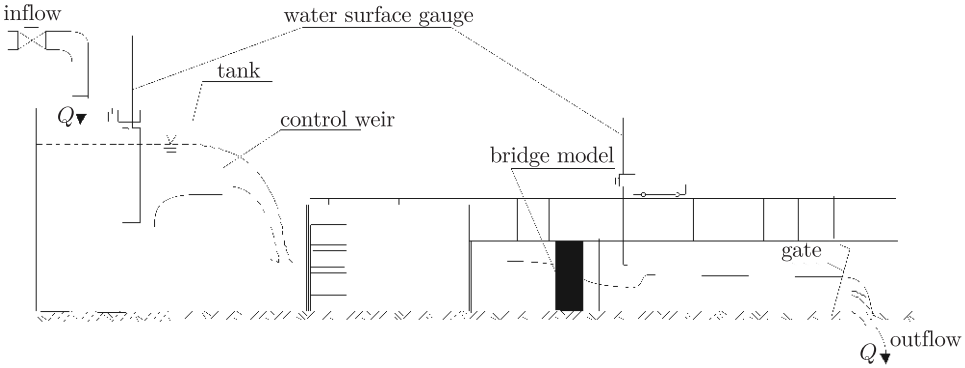

Figure 2. Schematic of the laboratory set-up

The steady flow in the laboratory hydraulic system was controlled with a weir at the inlet of the channel. For each experiment, the water discharge was equal to 0.114 m^3/s. The bottom of the channel was rigid, flat and horizontal. The water depth was controlled with a gate located at the outlet of the channel. In order to analyze the flow through the bridge section, two experiments were carried out. Photographs of the hydraulic phenomena observed during the experiments are shown in Figures 4 and 5.

In the first test, a depth of 0.48 m was imposed at the outflow section. This resulted in subcritical flow along the channel and in deflection of the water surface in the vicinity of the piers. In the second test, when the water depth at

Figure 3. General view of the laboratory channel and the bridge model

Figure 4. First experiment – subcritical flow

Figure 5. Second experiment – transcritical flow

the outflow was equal to 0.19 m, transcritical flow was observed in the channel. Upstream of the bridge, subcritical flow was observed. Along the constriction section (between the piers), a sudden decrease in the water surface occurred, making the flow supercritical. The flow near the outflow from the channel was subcritical again. This led to the formation of hydraulic jumps downstream of the bridge model. Moreover, we observed local phenomena accompanying the supercritical flow behind the piers, such as zones of diffraction and interference of abrupt swellings and depressions of water surface. These effects, merging in

space, were present almost along the entire length of the channel segment with supercritical flow.

4. Numerical simulations

In order to simulate two-dimensional water flow in the channel with a cross-section constricted by bridge piers using the FVM, the geometry of the channel was transformed into a numerical mesh. The 4-meter long flow domain was covered with an unstructured triangular mesh made of 8451 computational cells (Figure 6). The length of the side of a standard triangle was equal to 0.03 m, except for the area near the bridge. In order to ensure high resolution of the calculations in this rapidly changing flow area, the mesh was locally refined. The edges of the cells adjacent to the bridge piers were 0.01 m long. The areas inside the contours of the piers were excluded from the computational domain as a consequence of the closed boundaries imposed around the bridge piers.

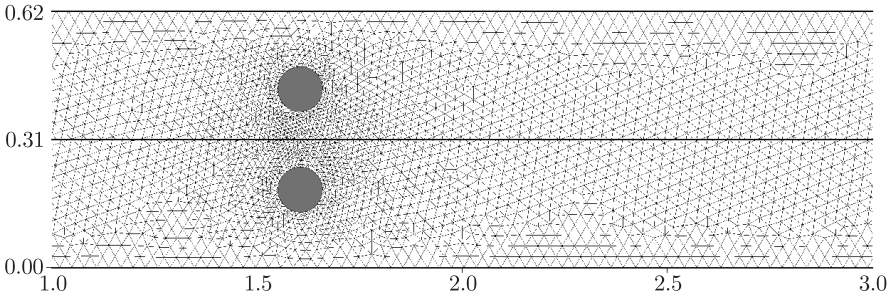

Figure 6. Fragment of the numerical mesh (dimensions in metres)

The remaining boundary conditions were also imposed in accordance with the laboratory experiment. The channel walls were treated as closed boundaries and the free slip condition was employed. At the inflow and outflow cross sections open boundary conditions were employed. At the inlet of the channel, the measured flow discharge was imposed as an upstream boundary condition, and at the outlet the water depth was imposed. The laboratory experiments of flow through the channel constriction were simulated numerically, starting from the steady uniform flow computed for the prismatic channel. Subsequently, if the obstruction was present in the channel, the computed flow parameters became unsteady for a moment due to the formation of a backwater profile upstream of the bridge and of a surface depression and hydraulic jump downstream of the piers. After several seconds, the simulated flow could be assumed to be steady. The calculations were carried out with a time step of $\Delta t = 0.001$ s. The total simulation time was 10 s in all cases.

The first numerical simulation corresponded to the first laboratory experiment. During this experiment, the flow was subcritical along the channel and the constriction. The comparison between the calculated (solid line) and measured (crosses) depth along the channel axis and the pier axis is shown in Figure 7.

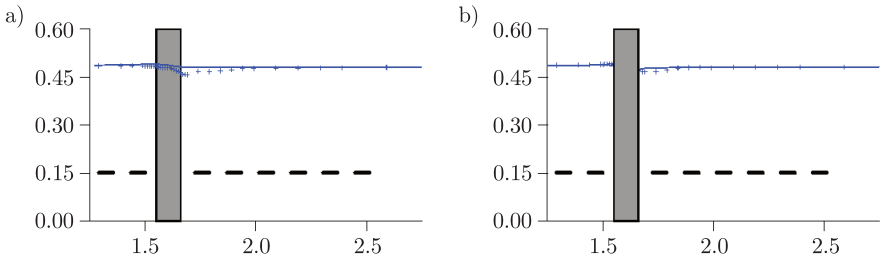

Figure 7. Measured (+ + +) and calculated (——) water surface profile for the first experiment together with the critical depth line (– –): a) along the channel axis, b) along the pier axis (dimensions in metres)

The agreement between these results is satisfactory for the water surface profile along the pier axis (Figure 7, panel (b)). In front of the pier, the surface rose, which was observed during the laboratory experiment. The computed water depth right behind the pier was also in agreement. There was an area of flow circulation where the water depth was lower than upstream of the bridge. Downstream of this "shadow zone", the water surface rose back to the normal depth controlled by the outflow gate. When the water surface profile along the channel axis (between the piers) was analyzed (Figure 7, panel (a)), a discrepancy between the computed and measured results was observed. The deflection of the water surface was also simulated along the constricted section of the channel, since the calculated water depth is generally overestimated there.

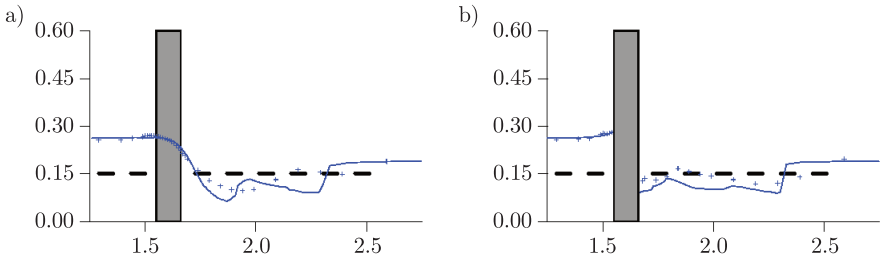

Figure 8. Measured (+ + +) and calculated (——) water surface profile for the second experiment together with the critical depth line (– –): a) along the channel axis, b) along the pier axis (dimensions in metres)

In the second numerical test, the transcritical open channel flow was simulated, corresponding to the second laboratory experiment. Here, the depth measurements were not very precise due to the water surface oscillations and the reflection of surface waves in the area of transcritical flow. A complex structure of shocks and depressions of the water surface could be observed along the channel between the piers and in the zone of the hydraulic jump. The local hydraulic effects merging in space made it difficult to carry out the measurements using simple laboratory equipment, such as the gauging needle. With this in mind, we note that the computed results were in qualitative agreement with the observations and (Figure 8). The water surface profiles upstream of the bridge section were

well-simulated both along the channel axis (Figure 8, panel (a)) and along the pier axis (Figure 8, panel (b)). For each profile, the water surface rose in this area resulting in a local swelling in front of the bridge. The shape of the water surface between the piers was simulated satisfactorily. Figure 8, panel (a) shows that the location of the crossing point with the critical depth line was correctly predicted to lie just downstream of the constriction, where the transition of the flow from subcritical into supercritical occurred. A discrepancy between the calculated and measured water depth in the channel section with supercritical flow can be observed. However, bearing in mind the limitations of the measurements, in this case, the simulated flow can still be deemed in qualitative agreement with experiment. Moreover, the transition of the second flow from supercritical to subcritical was simulated quite precisely. The hydraulic jump which formed downstream of the bridge section can be seen in Figure 8 as a sudden increase in the water depth, which became higher than the critical depth. The location of the hydraulic jump as well as the water depth near this local effect were also predicted quite well.

In addition to the one-dimensional analysis of water profiles along the channel, a two-dimensional numerical simulation allows us to compute the spatial distribution of flow parameters in the vicinity of the bridge. Figure 9 shows the water surface profile along the channel axis and the distribution of water depth computed in the second numerical simulation.

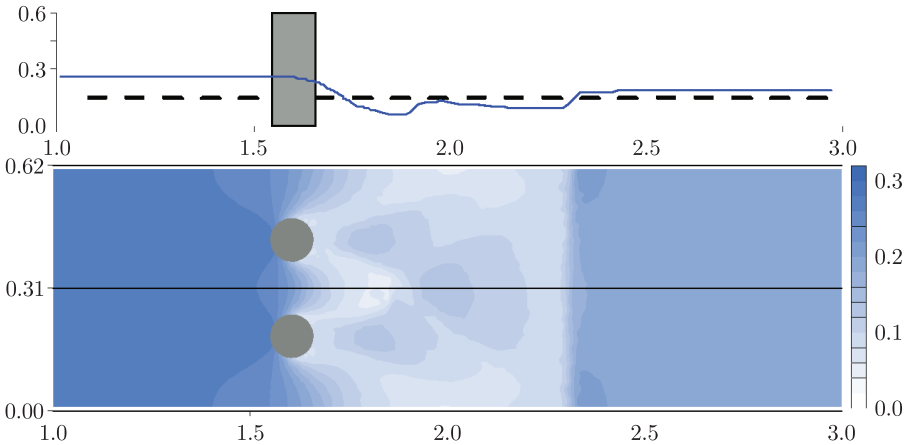

Figure 9. Surface profile and horizontal distribution of the computed water depth (dimensions in metres)

Furthermore, two-dimensional numerical simulations provide more information about the parameters of water flow. For instance, Figures 10 and 11 show the spatial distributions of flow velocity magnitude and of the values of the Froude number, respectively. The analysis of the numerical results presented in these figures and their comparison with the photographs taken during the experiment (Figure 5) showed that the main hydraulic characteristic of water flow in the

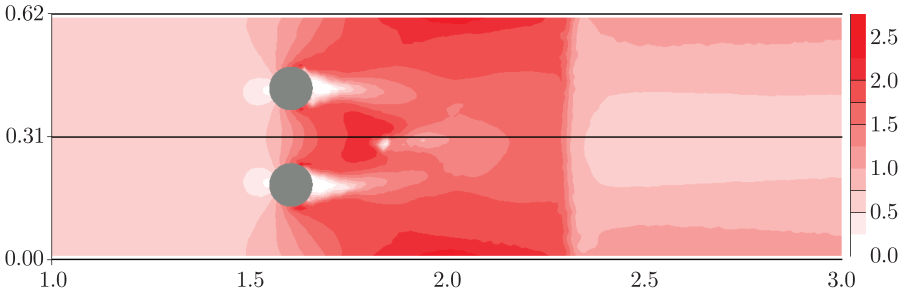

Figure 10. Distribution of flow velocity (m/s) (dimensions in metres)

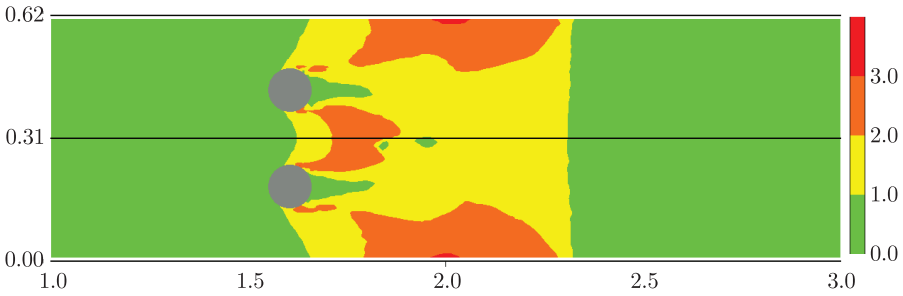

Figure 11. Spatial distribution of the Froude number (dimensions in metres)

vicinity of bridge piers model was correctly approximated. The water swellings in front of the piers, as well as the sudden lowering of the surface along the bridge cross-section are shown in Figure 9.

This figure reveals the complex structure of the surface waves merging downstream of the constriction. The simulated and observed locations of these local effects were also in good agreement. The calculated shape of the water surface in the area of supercritical flow (between the bridge and the hydraulic jump) was in agreement with experiment, which was verified by an examination of the water profiles along the channel walls and the axis as well as behind the piers. The water surface along the walls had the form of a long deflection without any additional wave effects between the bridge and the hydraulic jump. This was also observed in the laboratory channel. Upon the examination of the water profile along the channel axis, a sudden decrease right downstream of the bridge was observed. Further, in the same line, one wave crest was observed upstream of the hydraulic jump. It was located at about $x = 2\,\mathrm{m}$ and it was also present during the experiment. Analyzing the shape of the water surface behind the pier, we observed a local depression. In this area, flow circulation was observed. Along the pier axis, downstream of the pier, one wave crest was observed. It was located closer to the bridge section than the wave formed along the channel axis. Similar phenomena were observed in the laboratory channel. The complex structure of the flow between the bridge and the hydraulic jump resulted from the diffraction and interference of abrupt swellings and depressions of the water surface in the area of rapidly changing flow. There are two basic types of local

effects occurring due to the constriction of the channel cross-section. Oblique shocks consist in the sudden increase in water depth, together with a decrease in flow velocity; while depressions are associated with flow acceleration. Complex effects occurring locally downstream of the bridge are the result of superposition and interpenetration of the basic phenomena [9].

The flow near the bridge piers in the area of transcritical water motion can be also described by analyzing the velocity and the spatial distribution of the Froude number (Figures 10 and 11). The velocity magnitude field corresponded to the distribution of water depth (Figure 9). Wherever surface swellings, oblique shocks and hydraulic jumps occurred, there was a corresponding reduction in velocity. A decrease in velocity was also observed behind the piers in the "shadow zones" of water circulation. In the areas of water depressions, a decrease in water depth was accompanied by flow acceleration. The relationship between the flow velocity and water depth can be presented as the Froude number (*cf.* Figure 11), whose distribution rather precisely defines the spatial structure of transcritical flow, giving information about the locations of subcritical and supercritical flow zones and about the positions of hydraulic local effects accompanying flow transitions.

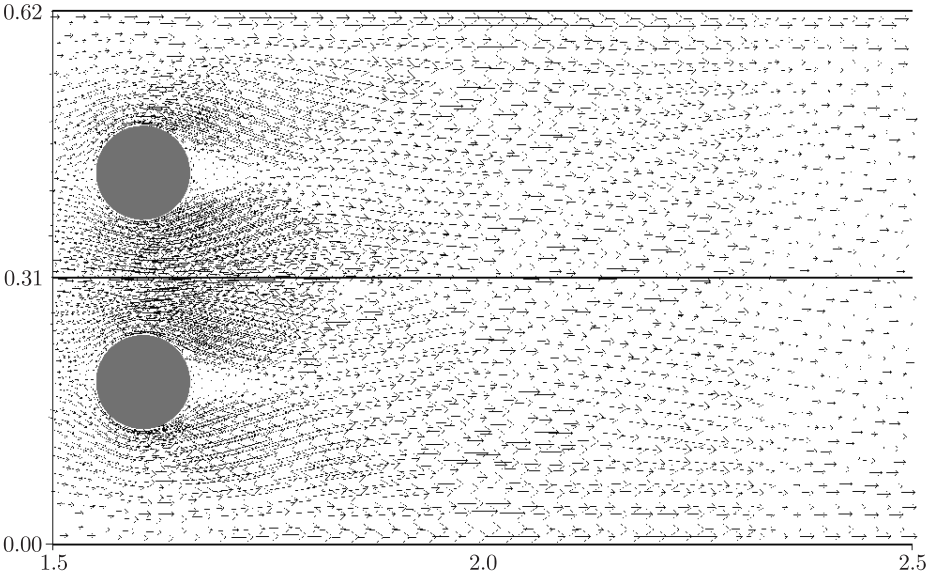

Figure 12. Depth-averaged velocity vectors $V_{\max} = 2.5\,\mathrm{m/s}$ (dimensions in metres)

In order to analyze the water flow between the bridge piers in more detail, the velocity vector field can be studied (Figure 12). For the second numerical simulation, the direction of the flow agreed well with experiment. In the cross-section of the bridge, where the reduction of the channel cross-section due to the presence of piers took place, acceleration of water flow was observed. The analysis of velocity vectors showed that the curvature of the streamlines was significant in

this constriction area. Downstream of the bridge, the streamlines became parallel to each other and to the channel walls. Finally, there was a decrease in velocity in a short section where the hydraulic jump formed. Behind the piers, the velocity was also approximated quite well. Still water zones bounded by high velocities of flow between obstacles were observed.

5. Conclusions

The results of two-dimensional numerical simulations of flow in the vicinity of bridge piers on a fixed channel bottom were presented in this paper. The following conclusions can be drawn.

- The shallow water equations can be successfully used to model the steady flow between the bridge piers. The results of the flow simulations through the constriction of the open channel were in good agreement with the measurements of the water surface profiles in the laboratory channel. In spite of the simplifications in the hydrodynamic model, local hydraulic effects in the area of transcritical flow were approximated satisfactorily. Of course, the inner structure of the local flow phenomena was lost due to the averaging of flow parameters during the derivation of the SWE model.
- The two-dimensional free-surface flow model can also be applied in order to simulate unsteady water motion. The satisfactory simulation results obtained for the steady flow through the local constriction hint at possible application of the SWE model to the analysis of flood hydrodynamics, where sudden reductions of the flow area are common. For instance, the inundation of river floodplains can result from the rising backwater profile upstream of a bridge section during flood wave propagation. Flood wave propagation in the river bed and the simulation of floodplain inundation can be carried out integrally using a two-dimensional model.
- The correct description of local effects in the simulation of transcritical flow near the bridge piers means the SWE model is a good candidate for modeling the integrated hydrodynamics of stormwater flow in urban areas. Stormwater systems consist of open channels, pipelines, reservoirs and natural creeks. Of course, if the flow capacity of the system is insufficient, flooding becomes possible. It seems that the SWE model can be satisfactorily used to model all surface-flow elements.

Acknowledgements

The author would like to acknowledge the financial support by the Polish National Science Center for the research project No. N N523 745840.

References

[1] Cunge J A, Holly Jr F M and Verwey A 1980 *Practical Aspects of Computational River Hydraulics*, Pitman, London
[2] Chow V T 1959 *Open-Channel Hydraulics*, McGraw-Hill Book Company, New York
[3] Pasiok R and Stilger-Szydło E 2010 *Arch. Civ. Mech. Engng* **10** (2) 67

[4] Huang W, Yang Q and Xiao H 2009 *Computers & Fluids* **38** (5) 1050
[5] Szydłowski M 2007 *Monographs of Gdansk University of Technology*, Gdansk **86** (in Polish)
[6] Abbott M B 1979 *Computational Hydraulics: Elements of the Theory of Free-Surface Flows*, Pitman, London
[7] Toro E F 1997 *Riemann Solvers and Numerical Methods for Fluid Dynamics*, Springer-Verlag, Berlin
[8] LeVeque R J 2002 *Finite Volume Method for Hyperbolic Problems*, Cambridge University Press, New York
[9] Causon C, Mingham C G and Ingram D M 1999 *J. Hydraul. Engng* **125** (10) 1039